Polymer 282 (2023) 126087

Contents lists available at ScienceDirect

Polymer

journal homepage: www.elsevier.com/locate/polymer

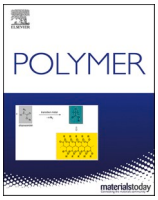

Polymer co-crystallization from LLE: Crystallization kinetics of POCB hydrate from two-phase mixtures of POCB and water

Sudesna Banerjee [a], Michael Gresh-Sill [a], Emily F. Barker [b], Tara Y. Meyer [b], Sachin S. Velankar [a,c,*]

[a] Department of Chemical Engineering, University of Pittsburgh, Pittsburgh, PA, 15260, USA
[b] Department of Chemistry, University of Pittsburgh, Pittsburgh, PA, 15260, USA
[c] Department of Mechanical Engineering and Materials Science, University of Pittsburgh, Pittsburgh, PA, 15260, USA

A B S T R A C T

Polyoxacyclobutane (POCB, $-[CH_2CH_2CH_2O-]_n$) has the rare ability to co-crystallize with water to form a hydrate. Above the melting point of the hydrate (~37 °C), mixtures exist in liquid-liquid equilibrium (LLE) between a POCB-rich and a water-rich liquid phase over a wide range of POCB:water ratios. Such phase behavior, which combines liquid-liquid equilibrium (LLE) and co-crystallization of a polymer with a small molecule, appears to be unique to POCB-water mixtures. Here, we examine the kinetics of isothermal hydrate co-crystallization when mixtures that are initially in liquid-liquid equilibrium (LLE) are cooled to below the hydrate melting point. Hydrate co-crystallization requires both POCB and water, and hence, it is coupled with transport of species between the liquid phases. Optical microscopy shows that hydrate crystallization occurs within the POCB-rich domains, and hydrate spherulites grow at constant speed. The temperature-dependence of the speed of hydrate growth front is consistent with the Hoffman Lauritzen model for homopolymer crystallization. Dilatometric measurements of bulk co-crystallization kinetics are conducted with constant stirring to avoid gravitational separation of the liquid phases. The temperature-dependence of bulk crystallization kinetics of these stirred mixtures in LLE is found to be far weaker than that of spherulitic growth kinetics, or of the quiescent bulk crystallization kinetics of mixtures starting from homogeneous conditions.

1. Introduction

Polyoxacyclobutane (POCB), with a repeat unit of $-[CH_2CH_2CH_2O-]_n$, is a semicrystalline polymer from the polyoxyalkylene series. It's known to form four polymorphs upon crystallization. Remarkably one of these polymorphs (originally called modification I) is a crystalline hydrate with a water/mer ratio of 1:1 [1–5]. Even though many polymers can be co-crystallized with small-molecule compounds [6–13], the co-crystallization of a polymer with water is rare and, thus far only known for POCB [1], linear polyethyleneimine [14], and possibly poly(1,3-dioxolane) [2,15,16]. Although the formation of a crystalline hydrate indicates a specific affinity for water, in fact, POCB is a hydrophobic polymer as judged by the fact that above the hydrate melting temperature, POCB/water mixtures can exist in a liquid-liquid equilibrium (LLE) state indicating incompatibility with water [4,5,17]. This study focuses on the kinetics of crystallization of POCB hydrate starting from the LLE state.

Previously, we examined the phase behavior of mixtures of POCB (M_n = 650 Da) and water [4,5]. Fig. 1 shows the temperature-composition phase diagram of POCB-water hydrate where the crystalline solid hydrate is denoted by the vertical solid line labeled Sc. At this molecular weight, the melting point of the hydrate (T_m = 37 °C) exceeds the melting point of both the constituents, pure POCB and pure water. For $T < T_m$, mixtures dilute in water show coexistence between the solid hydrate and POCB-rich liquid phase (Lp), whereas mixtures rich in water show coexistence between the solid hydrate and water-rich liquid phase (Lw). For $T < T_m$, mixtures dilute in water exist as a homogenous liquid state (Lp), whereas water-rich mixtures show liquid-liquid equilibrium (LLE) between the Lp and Lw phases. The original experimental data supporting this diagram, along with a longer discussion, are available in Banerjee et al. [5]

We now turn from the phase diagram to kinetics of hydrate crystallization when an initially-liquid mixture is cooled from above the melting temperature T_m to below it. Fig. 1 immediately suggests that for such a cooling process, hydrate crystallization may occur either from a homogeneous liquid state or from an LLE state. As discussed previously [4], three cooling trajectories (blue arrows in Fig. 1) can be identified. The leftmost arrow labeled A corresponds an initially-homogenous

* Corresponding author. Department of Chemical Engineering, University of Pittsburgh, Pittsburgh, PA, 15260, USA.
E-mail addresses: sub66@pitt.edu (S. Banerjee), gresh033@umn.edu (M. Gresh-Sill), emily.barker@pitt.edu (E.F. Barker), tmeyer@pitt.edu (T.Y. Meyer), velankar@pitt.edu (S.S. Velankar).

https://doi.org/10.1016/j.polymer.2023.126087
Received 12 April 2023; Received in revised form 2 June 2023; Accepted 4 June 2023
Available online 15 June 2023

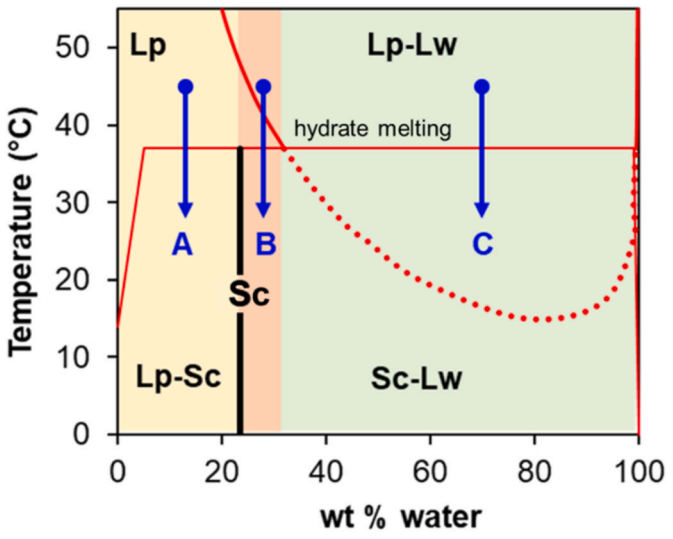

Fig. 1. Phase diagram for 650 Da POCB and water reproduced from Ref. [5]. The vertical black line labeled Sc indicates the composition of the co-crystal hydrate. The solid red line indicates liquid−liquid coexistence between Lp and Lw phases. The dotted red line indicates a metastable portion of the liquid−liquid coexistence curve. Blue arrows labeled A, B, and C illustrate cooling samples in three different composition regions (see text for discussion). The left boundary of the Lp−Sc region is drawn approximately since, in principle, there must be triple point coexistence of Lp, Sc and solid POCB at some low water content as discussed in Banerjee et al. [5]. This complexity does not affect this paper. (For interpretation of the references to colour in this figure legend, the reader is referred to the Web version of this article.)

liquid mixture which forms solid hydrate upon cooling below T_m. The uncrystallized portion of the mixture becomes increasingly depleted in water as the hydrate crystallizes but remains a homogeneous liquid throughout. This situation was examined in our previous article [4] (details in the next paragraph). The rightmost arrow labeled C corresponds to crystallization upon cooling a two-phase mixture that is initially in Lp−Lw coexistence. Since the initial liquid mixture has a lower POCB fraction than the hydrate, the uncrystallized portion of the liquid mixture becomes increasingly depleted in POCB as crystallization proceeds but remains in LLE during all or most of the crystallization process. This case is the focus of the present study. The arrow labeled B is more complex since the mixture is single phase immediately above T_m, but LLE may be induced by hydrate formation.

In our previous study [4] of crystallization kinetics for the cooling trajectory A of Fig. 1, initially homogeneous liquid mixtures of POCB and water were cooled rapidly from 48 °C (above T_m) to a temperature $T_c < T_m$ and then allowed to crystallize under isothermal conditions. Experiments examined the kinetics of bulk crystallization of hydrate by dilatometry as well as the speed of the spherulites growth front by optical microscopy, both under quiescent conditions. The main results of the paper were (1) bulk crystallization as well as the speed of the spherulite growth front became slower as T_c increased, in a manner consistent with the Hoffman-Lauritzen model for homopolymer crystallization, (2) crystallization also became slower as the mixtures became more dilute in water, (3) spherulite growth speed decreased as the spherulites grew, especially in mixtures with low water content, and (4) quiescent bulk crystallization kinetics broadly followed the Avarami model where the Avarami exponent was found to decrease with increasing temperature [4]. To our knowledge, this was the first systematic study of cocrystallization kinetics of a polymer with a small molecule. Broadly we concluded that the hydrate cocrystallization kinetics are similar to homopolymer crystallization, but with the additional complexity that as the mixture composition deviates from the hydrate composition, the species in excess (POCB in our case [4]) is rejected from the crystal. This creates diffusion limitations to crystallization, analogous to the effect of an impurity in homopolymer crystallization [18].

The objective of the present study is to quantify hydrate crystallization kinetics for the cooling trajectory C. Several key differences may be expected for such crystallization-from-LLE as compared to our previous [4] work on trajectory A. First, crystallization may occur in one or both liquid phases, or at the interface, at different rates. Second, since the liquid phase compositions are different from the hydrate composition, hydrate crystallization must be accompanied by interfacial mass transport as the system seeks to maintain equilibrium between the uncrystallized liquid phases. Indeed, if crystallization at the interface is rapid, the interface may turn solid and prevent further crystallization by blocking interfacial mass exchange. Finally, and most importantly, since the POCB-rich phase is denser than the water-rich phase, gravity can induce layering of the two liquid phases. Thus, the crystallizing mixture must be stirred continuously, otherwise the kinetics would depend on the extent to which such layering occurred.

Some of the above complexities appear specifically because of the coupling between LLE and cocrystallization. While there are many examples of cocrystallization of polymer with a small-molecule species [6–13], we are unaware of any other examples where co-crystallization and LLE appear simultaneously. Therefore, some of these issues may be unique to the POCB/water system. Some of the other complexities, e.g. the importance of stirring or of the relative rates of crystallization vs LLE, also appear when a homopolymer crystallizes out of a two-phase solution with a small-molecule solvent [19–24].

Incidentally, crystallization of fully- or partially-immiscible homopolymer blends [18,25–27] also involves crystallization from LLE, but the above complexities do not appear. High bulk viscosity of molten polymers makes gravitational effects negligible, and stirring is not needed. Most polymer blends are fully-immiscible and hence crystallization does not involve re-equilibrating the uncrystallized liquid phases [25]. Full immiscibility also implies that the overall mixture composition has little effect on crystallization. In partially immiscible polymer blends, LLE behavior can affect crystallization, however in those cases, the effect of partial miscibility on glass transition temperature is often the dominant effect [18,25,28].

2. Experimental section

2.1. Bulk crystallization kinetics of isothermal crystallization

The experiments in this section were conducted on POCB of a manufacturer-quoted molecular weight of 650 g/mol and is denoted as POCB650 [5]. Bulk crystallization kinetics was examined by dilatometry as in our prior work [4]. Mixtures of POCB650 and water were cooled rapidly from molten conditions at 48 °C to the desired crystallization temperature ($T_c < T_m$), and then crystallization was allowed to proceed isothermally. The resulting volume changes relate qualitatively to the kinetics of hydrate crystallization. The experimental procedure was nearly identical to the previous [4] study with the exception of stirring (next paragraph). The sample was placed in a dilatometer and covered by mineral oil which rose into the stem of the dilatometer tube. The dilatometer was first held at 48 °C, far above the melting point of the hydrate, and then quickly transferred to the isothermal bath already set to the fixed crystallization temperature T_c (range 26 °C–33 °C). Changes in the oil level due to crystallization were recorded and a snapshot from the video is shown in ESI Figure S1. Three independently prepared samples of the same composition were examined at various temperatures, and exemplary data for the volume change vs time are shown in the Supplementary Fig. S2.

Experiments were conducted at a mixture composition of 20 wt% POCB650, 80% water. This composition was selected as a tradeoff between ease of stirring and ease of measurement. As explained above, crystallization from an LLE state requires continuous stirring which is

only possible at low POCB content. At high POCB content, the mixture develops a pasty consistency due to the high-volume fraction of solid hydrate making it difficult to maintain continuous stirring. On the other hand, low POCB content corresponds to low volume change due to crystallization, thus reducing the accuracy of dilatometry. The composition of 20% POCB was selected as a tradeoff between the two factors: keeping the mixture freely flowing up to the end of crystallization, while also retaining a volume change that was easily quantifiable.

As mentioned in Section 1, in the absence of stirring, the mixture separates into two liquid layers prior to crystallization [5]. As observed previously [5], under quiescent conditions, crystallization proceeds relatively rapidly near the interface (since water and POCB are both needed for hydrate formation) whereas the bulk of the two phases crystallize slowly, if at all. Accordingly, all experiments in this paper were conducted by adding a small magnetic stir bar to the dilatometer to ensure that the two phases remained well-mixed, and there are negligible composition gradients within the bulk liquid phases. In fact, Fig. S3 shows that without stirring, crystallization proceeds much more slowly as compared to continuous stirring.

Volume contraction was observed to happen in two stages: an initial volume contraction due to cooling of the sample from 48 °C to T_c, and a subsequent contraction due to crystallization. Therefore, the volume change due to crystallization was calculated from Eq (1).

$$\Delta V_c(t) = -\left(\Delta V_{total}(t) - \Delta V_{tc}(t)\right) \quad \text{Eq 1}$$

The subscripts tc and c refer to "thermal contraction" and "crystallization," respectively. The negative sign ensures that $\Delta V_c(t)$ is presented as a positive value. The value of $\Delta V_{total}(t)$ was obtained from the analysis of the experimental videos. The procedure for obtaining $\Delta V_{tc}(t)$ was described previously [4]. The $\Delta V_c(t)$ thus estimated from Eq. (1) was then normalized by the sample mass to give the specific volume change of crystallization, $\Delta v_c(t)$, which is shown in Fig. 2.

At any specific T_c value, Δv_c vs log(t) has a sigmoidal shape where Δv_c remains near zero for some initial "induction period", followed by an increase in Δv_c towards its final value. Fig. 2 shows that the final value is nearly temperature-independent, whereas the time needed to approach this final value reduces sharply with decreasing temperature.

The experimental volume change at long time can be compared with the theoretical volume change (assuming complete crystallization of all POCB) $\Delta v_c^{\max}$, which is given as

$$\Delta v_c^{max} = \left(\frac{m_{POCB}}{\rho_{POCB}(T)} + \frac{1-m_{POCB}}{\rho_{water}(T)}\right) - \left(\frac{m_{POCB}/0.764}{\rho_c} + \frac{1-m_{POCB}/0.764}{\rho_w}\right) \quad \text{Eq 2}$$

Here, ρ_w, ρ_{POCB}, *and* ρ_c are the densities of the water, POCB650, and hydrate crystal respectively, m_{POCB} indicates the mass percentage of POCB in the mixture, and 0.764 is the mass fraction of POCB in the crystal (corresponding to 1:1 M ratio of monomer to water). Here, the first bracket is the specific volume of the liquid prior to crystallization (assuming no volume change of mixing), and the latter bracket is the sum of the volumes of the crystal and the uncrystallized POCB. The density of the crystal, estimated from the dimensions of the unit cell [1], is $\rho_c = 1.176$ g/mL, whereas $\rho_{POCB} = 1.02$ g/mL and $\rho_w = 1.00$ g/mL. All three densities are taken as independent of temperature. Using Eq (2), and with $m_{POCB} = 0.2$, the theoretical volume change (Δv_c^{max}) is found to be 0.0353 mL/g. This value is nearly two-fold larger than the final value in Fig. 2 suggesting that only roughly half of the total sample crystallizes. In fact the previous study [4] on homogeneous crystallization also showed a similar two-fold mismatch between the measured volume change at long times and Δv_c^{max}. As with homopolymer crystallization, we believe that chain defects and chain ends may be the reason underlying incomplete crystallization.

We note that the Δv_c^{max} calculated from Eq (2) is sensitive to any inaccuracies in ρ_c . In fact, using $\rho_c = 1.14$ g/mL (rather than 1.176 g/mL) brings the prediction of Eq (2) close to the experimental results. Similarly, Eq (2) neglects any volume change of mixing which may further affect Δv_c^{max}.

We now turn to the time dependence of $\Delta v_c(t)$ in Fig. 2 which reflects kinetics of the crystallization process. As a simple way to capture the kinetics, we report the time τ at which Δv_c reaches the value of 0.005 mL/g (chosen arbitrarily). The dependence of τ on T_c is shown in Fig. 3 (the three symbols indicate three independently-prepared samples). As expected from the literature on homopolymer crystallization, crystallization accelerates significantly with reducing crystallization temperature. In Section 3, we will compare this temperature dependence of τ against our previous results for quiescent crystallization from a single-phase liquid state.

We also considered a second way to quantify kinetics. Fig. 2 clearly shows that Δv_c remains nearly zero for a certain period, often called the induction time. This induction time, t_{ind} has been regarded as the time for primary nucleation [29] and serves as another measure of crystallization kinetics. To obtain t_{ind}, the data of Fig. 2 were fitted to the Avrami equation [30]:

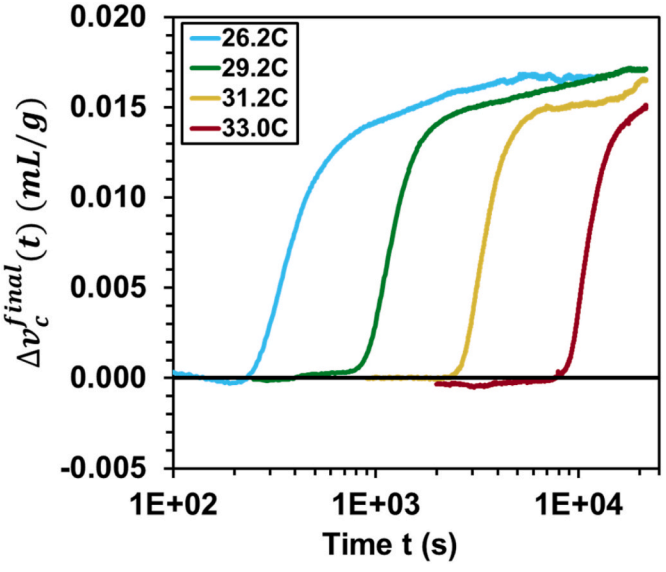

Fig. 2. Specific volume changes due to crystallization at different crystallization temperatures of a mixture with $m_{POCB} = 0.2$.

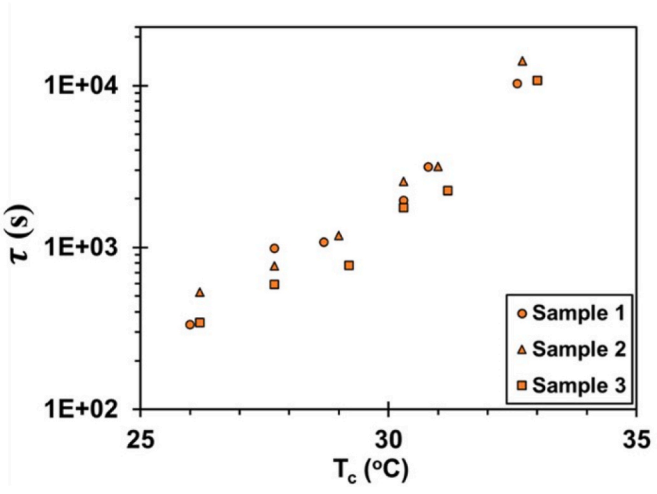

Fig. 3. Time τ required to reach $\Delta v_c = 0.005$ mL/g vs crystallization temperature. The three symbols refer to independently prepared samples, all with 20 wt% POCB.

$$\Delta v_c = \Delta v_c^{final}\left(1 - \exp\left(-k(t - t_{ind})^n\right)\right) \quad \text{Eq 3}$$

where n is the Avrami exponent, k is the Avrami coefficient, Δv_c^{final} is the volume change at long times. We acknowledge that the central assumptions of Avrami equation are not valid here since the samples are in LLE and under constant stirring. Accordingly, no physical significance can be attributed to n; we use Eq (3) solely as a means of fitting the $\Delta v_c(t)$ data to estimate t_{ind} consistently across all samples. The data were fitted in a linearized form using Δv_c^{final}, k, t_{ind}, and n as fitting parameters. The resulting fits are shown in linearized form, in ESI Figure S4a. The values of Avrami exponent (n) vary across a wide range from 1.5 to 3.8 and increase with T_c (ESI Figure S4b). These two measures of crystallization kinetics, τ and t_{ind} may now be compared.

Fig. S4c shows that the ratio τ/t_{ind} is typically about 1.5, albeit with significant variability, but there is no obvious trend with crystallization temperature. Thus, both measures of crystallization kinetics show roughly the same temperature-dependence, and hence we will only discuss τ later in this paper.

2.2. Local speed of spherulite growth front - in isothermal crystallization

Previously [4] we examined the dependence of the speed of the spherulite growth front on temperature for crystallization from a homogeneous liquid state, i.e. the blue arrow A in Fig. 1. In that case, spherulites nucleated and grew with time throughout the bulk of the sample. In the present case however, crystallization proceeds from an LLE state wherein drops of the POCB-rich phase are suspended in the water-rich phase with continuous stirring. Prior research [5] on the same POCB650 as used here showed that samples with as little as 0.1% POCB were in LLE suggesting that the solubility of POCB in water is less than 0.1%. Since the water-rich phase is nearly devoid of POCB, hydrate crystallization is expected to occur inside the drops of the POCB-rich phase, and result in globular crystals. Indeed mixtures containing 1 wt % POCB650 did show drops of the POCB-rich phase forming globular crystals [5]. Puzzlingly however, they were endowed with a corona of crystals suggesting that some hydrate crystallization could also occur in the aqueous phase immediately outside the drops. Thus, we sought to resolve this complexity before delving into measurements of spherulitic growth rates within the POCB-rich phase.

Samples with 20 wt% POCB650 were shaken vigorously and then allowed to crystallize quiescently. Surprisingly these samples showed two distinct morphologies (Fig. 4a). The first consists of hydrate globules as expected, and as previously [5], the globules are endowed with a corona of crystals. The second is loosely packed sheaf-like structures resembling spherulites crystallized from homogeneous solution. These two distinct structures, globules, and spherulite-like crystals, appear at all crystallization temperatures examined, ranging from 9 °C to 35 °C. The presence of the spherulite-like structure is puzzling because it is not clear how such a morphology, apparently untethered from any globules, would appear if the water-rich phase was nearly devoid of polymer.

We therefore hypothesized that a portion of the polydisperse POCB650 sample has sufficiently low molecular weight to be soluble in the water-rich phase. This soluble portion may then crystallize homogeneously to form the loose spherulite-like hydrate structures evident in Fig. 4a. This hypothesis was tested by extracting water-soluble and water-insoluble fractions from POCB650 and crystallizing them separately.

A schematic of the fractionation procedure is shown in ESI Figure S7. Briefly, a 10:90 mixture POCB and water was stirred at 40 °C and then allowed to settle under gravity. A portion of the supernatant water was extracted, filtered to remove any insoluble POCB droplets, and then dried in vacuum. This soluble portion comprised roughly 30% of the original POCB. A portion of the precipitated POCB was also extracted and dried in vacuum. Gel permeation chromatography (Fig. 4b) confirms that the average molecular weight increases in the order of soluble fraction, original POCB650, and the insoluble fraction. Note that the M_n values appear higher than expected because they are reported relative to polystyrene standards in which the lowest standard was 2500 g/mol. Therefore, the GPC-reported molecular weight of the POCB650 deviates somewhat from manufacturer-quoted value of 650 g/mol; the soluble

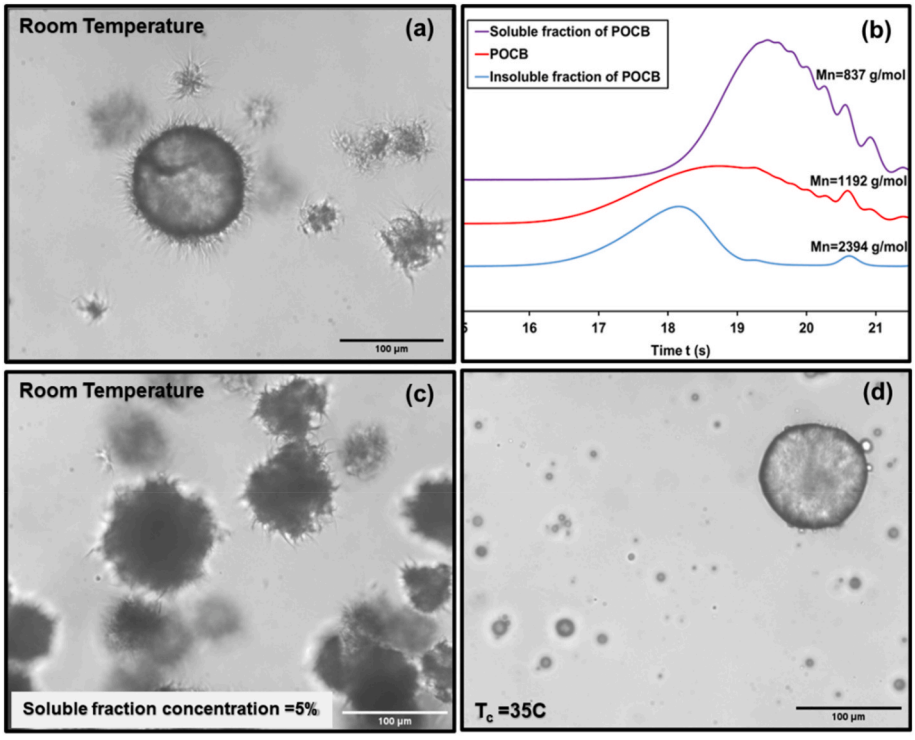

Fig. 4. (a) Microscopic structure of hydrate of unfractionated POCB650 in bulk water (b) GPC traces for soluble and insoluble fraction of polymer. (c) Hydrate crystallized from lower molecular weight polymer dissolved in aqueous solution (d) Hydrate crystallization from high molecular weight fraction dispersed in water.

and insoluble fractions are expected to exhibit a similar shift in GPC molecular weight.

The melting temperatures of these two fractions were measured by dispersing a small amount of each fraction into vials of water to form flakes of hydrate, and then heating the vials until the flakes melted completely. These values were found to be $T_m = 37$ °C for the soluble fraction, and 41 °C for the insoluble fraction.

Following fractionation, two separate mixtures were prepared: a homogeneous solution by dissolving the soluble fraction in water, and an LLE mixture by dispersing the insoluble fraction as droplets in water. The homogeneous mixture was cooled to room temperature and allowed to crystallize, whereas the LLE mixture was held at 35 °C until it crystallized. For the LCST-type LLE curve observed here, these crystallization temperatures guarantee that the fraction that was soluble at 40 °C remains fully dissolved, whereas the fraction that was insoluble at 40 °C remained nearly completely insoluble. Upon crystallization, the samples were imaged (Fig. 4c and d).

Loosely packed spherulite-like structures appear in Fig. 4c with no evidence of any hydrate globules. In contrast, Fig. 4d only shows hydrate globules but no spherulite-like structures suggesting that there was no crystallization in the aqueous phase; instead, crystallization only occurred by water diffusing into initially-spherical drops of the POCB-rich phase. These images strongly support the idea that it is the soluble portion of the POCB650 that creates the spherulite-like hydrate structures. Incidentally it is noteworthy that the globule in Fig. 4d lacks a corona. This suggests that the corona in Fig. 4a was formed by the soluble portion of the POCB crystallizing as a hydrate onto the surface of the globules.

We now turn to a microscopic study of crystallization speed, Guided by the results of polydispersity effects, two separate studies were conducted, one examining the crystallization of the soluble fraction from homogeneous mixtures, and another examining the crystallization of the insoluble fraction from mixtures in LLE.

The soluble fraction was dissolved in water at 4 wt%, cooled from 48 °C to the desired crystallization temperature, and allowed to crystallize isothermally. The growth of the spherulite-like structures was monitored by optical microscopy, and the time-evolution of the speed of the growth front G is shown in Fig. 5a at various temperatures. Each curve corresponds to a single spherulite-like structure, and in many cases, G decreased as the crystallization progressed. Eventually crystallization must stop as the polymer in the bulk is exhausted and hence G must approach zero, but our experiments were not conducted to that point. This is because at such late stages when the spherulite-like structures are relatively large, they often move, e.g., by rolling over due to gravity and it is difficult to follow their growth in a consistent manner. The decrease of speed in growth at early times in Fig. 5a may be attributed to the overall depletion of the soluble POCB as crystallization proceeds. Diffusional limitations for the POCB to arrive at the crystal growth front may cause a further slowing down of the growth as the spherulite-like structures grow. There is significant variability in the G vs R behavior. Each of these spherulitic structures were recorded in the exact same experiment, thus ruling out temperature variation as the source of the variability. Typically, spherulites that grow later in the process grow more slowly than early-starting spherulites, and thus we believe that bulk depletion of POCB may be the reason for the variability. Further sources of variability may be the proximity of other spherulites; since nucleation density is low, a large spherulite may deplete the solution in its vicinity of POCB. Regardless, to approximately quantify the temperature-dependence of the speed of spherulitic growth, an arbitrary radius of R = 22 μm was chosen and Fig. 5b shows that the speed of growth front decreases as T_c increases.

We now turn to the insoluble fraction which, in the case of stirred POCB-water mixtures, forms POCB-rich drops which eventually crystallize into globules. It is difficult to measure G for crystallization inside of spherical droplets due to complications including the difficulty of observing crystallization growth fronts inside the spherical geometry of a drop, of nucleating a crystal inside very small drops, and of wetting of the drops onto the surface of the container used for microscopy. Accordingly, samples for this second study were prepared as follows. The insoluble fraction was dispersed into a large excess of water with gentle shaking. This dispersion was then spread onto a Petri dish where the individual drops of the POCB-rich phase sedimented and wetted the bottom surface to form shallow puddles fully-covered by a thick layer of the aqueous phase. These puddles, some of which spread over several hundred microns, could be observed readily by optical microscopy. The typical thickness of puddles, measured post-crystallization, was about 15–20 μm (ESI Figure S6). The dish was then cooled to the desired crystallization temperature upon which each puddle crystallized, typically starting from a single nucleation event within each puddle. The speed of crystallization growth was calculated by tracking the crystallization front with time. No significant change of G with time was found as the crystallization front advanced across the puddle. Fig. 6a shows the different stages of crystallization growth in the puddle. The speed of growth front G measured at different temperatures is shown in Fig. 6b and reduces with increasing T_c.

3. Discussion

We will now place the results of POCB hydrate co-crystallization in the context of the broader literature on homopolymer crystallization, compare the kinetics of this study against our previous measurements under homogeneous conditions, and compare the temperature-dependence of crystallization kinetics measured on the various samples by different methods.

For crystallization of homopolymers far above their glass transition temperature, the Hoffman−Lauritzen theory predicts

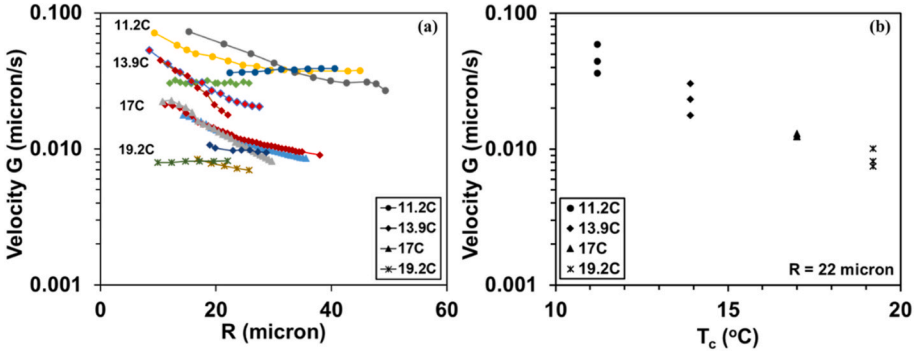

Fig. 5. Hydrate crystallization of the low molecular weight soluble fraction. (a) Growth speed for spherulite-like crystallization of the soluble fraction dissolved at 4 wt% loading in aqueous solution; (b) Temperature dependence of growth speed at when the size of the spherulite-like crystals is R = 22 μm.

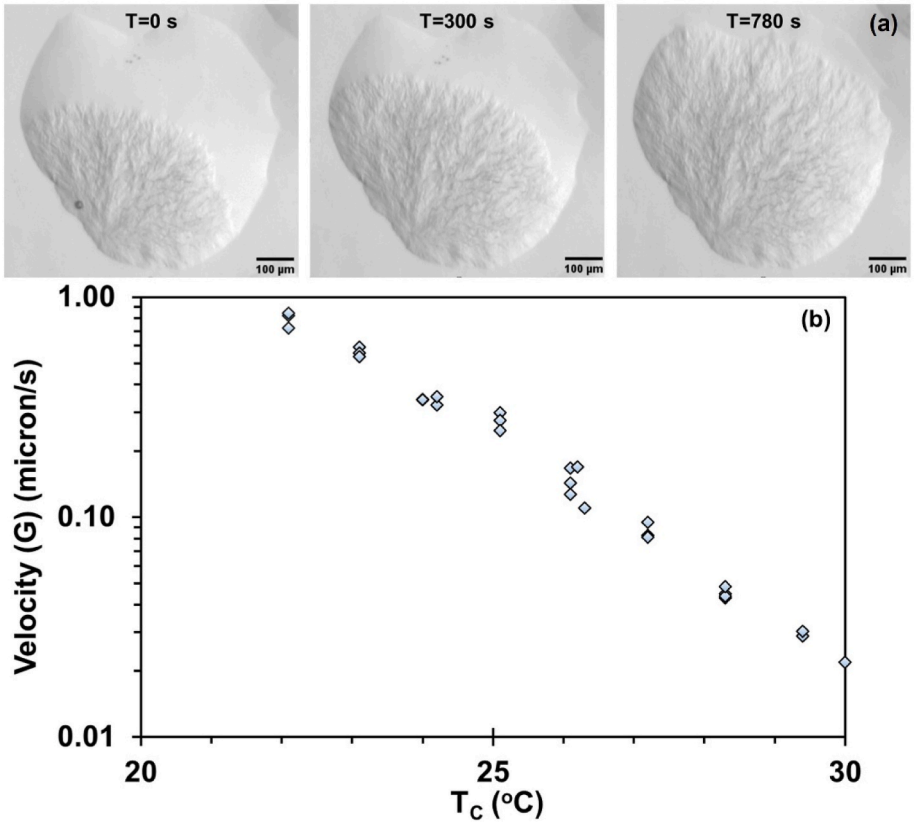

Fig. 6. Hydrate crystallization of the high molecular weight insoluble fraction. (a) Different stages of crystallization within a puddle (b) Crystallization growth speed vs. T_c. Each temperature corresponds to an independent experiment, whereas multiple points at an individual temperature correspond to different puddles observed in the same experiment.

$$\log_{10} G = A + B\left(\frac{T_m}{T_c \Delta T}\right) \quad \text{Eq 4}$$

where $\Delta T = (T_m - T_c)$ is the undercooling. Previously [4] we showed that for mixtures with 18% water which are homogeneous prior to crystallization, the speed of spherulite growth for quiescent crystallization agreed with Eq (4). Those data are shown as purple diamonds in Fig. 7.

Analogously, we now plot the growth speed data for the soluble fraction (open circles, same data as Fig. 5b), and the insoluble fraction (open diamonds, same data as Fig. 6b) on the same plot. Note that in Fig. 7, the experimental range of T_c is 284 K–305 K, compared with the melting temperature of 310 K for the soluble fraction and 314 K for the insoluble fraction. Accordingly, the ratio T_m/T_c is close to 1, and nearly invariant with temperature, i.e., the x-axis of Fig. 7 is nearly equal to 100/ ΔT.

The speed of spherulite growth for all three cases – the POCB650, the soluble fraction, and the insoluble fraction – can be fitted reasonably well with straight lines indicating that hydrate crystallization is well-described by Hoffman-Lauritzen model. The three corresponding values of the slope B in Eq. (4) span a modest range from -0.41×10^{-2} K^{-1} to -0.53×10^{-2} K^{-1}. Note that the three samples have large differences in composition. The open red circles have the highest water content (96 wt% water and 4% polymer). The purple diamonds have the lowest water content (18 wt% water and 72% polymer [4]). The water content of the open black diamonds (labeled insoluble fraction) is unknown since crystallization occurs within the puddles of the POCB-rich phase. Thus, the water content is governed by the solubility of water in the insoluble fraction of POCB which cannot be measured at the crystallization temperatures. It can however be estimated via cloud point measurements at 40 °C at which hydrate does not crystallize.

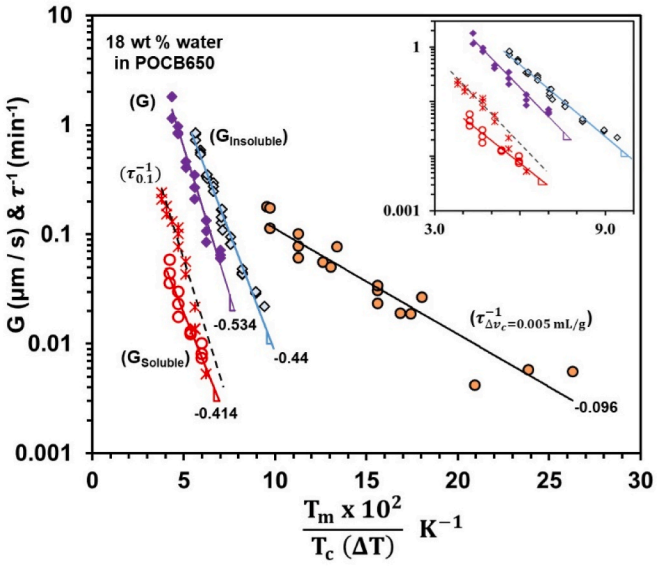

Fig. 7. Crystallization kinetics in Hoffman–Lauritzen form. Bulk crystallization kinetics:(✳) bulk quiescent crystallization of 72:18 mixture of POCB650 and water [4]; (●) bulk crystallization of 20:80 mixture of POCB650 and water with stirring. Spherulite growth speed: (◆) 72:18 mixture POCB650 and water [4]; (○) 4:96 mixture of soluble fraction of POCB650 with water; (◇) insoluble fraction of POCB650 in water. Numbers next to each line are values of B in Eq (4).(Inset shows a magnified view of some of the data).

Experiments [31] at 40 °C suggest that the solubility of water in the POCB-rich phase of the insoluble fraction is roughly 10 wt%. At crystallization temperatures, the solubility of water in the POCB is likely to be somewhat higher due to the LCST-type LLE. Thus, we tentatively estimate that the samples corresponding to the black diamonds have somewhat more than 10 wt% water. Despite this large difference in water content across the three samples, the temperature dependence of all three samples is nearly similar. Note however that the three samples also differ in molecular weight and cannot be compared readily with previous concentration studies [32–34] conducted at fixed molecular weight.

We now turn to the temperature-dependence of the isothermal bulk crystallization kinetics measured by dilatometry. Previously [4] we showed that at 18 wt% water under quiescent conditions starting from a homogenous mixture, the bulk crystallization kinetics had nearly the same temperature-dependence as G. Those data are shown as the red stars in Fig. 7. In stark contrast, for the samples with 80 % water crystallized from an LLE state, the bulk kinetics (the τ^{-1} data from Fig. 3, shown as filled orange circles) has a far weaker temperature-dependence than G.

We do not have any firm explanation for this weak temperature dependence, but some possible explanations may be ruled out. The central difference between the various samples in Fig. 7 is that the experiments leading to the filled orange circles were conducted with continuous stirring, whereas all the other experiments were under quiescent conditions. Previously we noted that under quiescent conditions, the uncrystallized POCB must diffuse away from crystallization front and create diffusion limitations to hydrate crystallization. Such diffusion limitations would disappear in the stirred experiments. However, diffusion limitations generally *reduce* the temperature dependence of crystallization growth processes [18,35] since diffusion has a weaker temperature dependence than nucleation. Clearly then, diffusion limitations cannot explain why the stirred samples have a weaker temperature dependence. A second difference is that stirring may induce continual breakage of crystals, especially at the earliest stages of crystal growth. This should increase the crystallization rate since there are now more locations for crystal growth, but it is not clear why crystal breakage should alter the temperature dependence. A third difference is specific to crystallization under LLE conditions. The phase diagram suggests that in both the coexisting liquid phase liquid phases, the water: polymer ratio is lower than the 1:1 molar ratio of water: monomer in the crystal. Since the hydrate crystallization proceeds within the POCB rich phase, this phase must get depleted of water. Accordingly, to maintain chemical equilibrium between the liquid phases as crystallization proceeds, the POCB-rich phase must gain water (it could also lose POCB, but we presume this would be slower than water transport). If this interfacial transport of water is much slower than crystal growth, the overall crystallization rate would be governed by the (weak) temperature-dependence of the interfacial transport. Stirring would reduce these transport limitations and hence strengthen the temperature-dependence. Once again, this is contrary to the data where the quiescent experiment with the insoluble fraction (open diamonds) has a stronger temperature dependence than the stirred sample (orange circles).

One speculation that may explain the weak temperature dependence of the stirred samples is that stirring greatly increases the secondary nucleation rate. Thus, if quiescent crystallization is in Regime I (secondary nucleation is the rate-limiting step, whereas the intrinsic speed of growth is much faster), stirring may take it to regime II (secondary nucleation becomes comparable to the intrinsic growth speed). This would decrease the temperature-dependence. This is well-known in homopolymers where increasing undercooling may cause a sharp decrease in the slope of the Hoffman-Lauritzen plot due to a Regime I to Regime II transition. We note however that such a transition is generally expected to have a 2x decrease in the temperature-dependence, whereas the slope of the stirred sample in Fig. 7 is at least 4x lower than of the quiescent samples. In summary, we are unable to conclusively explain the weak temperature of the bulk crystallization of the well-stirred samples.

The above discussion of interfacial transport of water raises the question about whether our spherulitic growth experiments in puddles were actually limited by water transport from the aqueous to the polymer-rich phase. As mentioned in Section 2.2, typical height of the puddles is $h = 15$–20 μm (see Fig. S6). Assuming the diffusion coefficient of water in POCB is similar to the water diffusivity D in PDMS [36,37] on the order of $10^{-9}\mathrm{m}^2/\mathrm{s}$, the diffusion time for water to equilibrate across a 20 μm thick puddle is $h^2/4D = 0.1\ s$. At the highest speed of growth reported in Fig. 6b ($G \approx 1$ μm/s) the growing crystallization front would move only 0.1 μm within the equilibration time, a distance that is far smaller than the puddle thickness. This calculation suggests the spherulitic growth was not limited by diffusion of water from the aqueous phase. This physical picture – that the water content of the POCB-rich phase remains at equilibrium and does not change during crystallization – is consistent with the observation that the G remains invariant as crystallization proceeds. In effect, the large pool of water serves as a "buffer" under these conditions. This is in contrast with hydrate crystallization from homogeneous mixtures [4] where one of the two species becomes depleted with time.

4. Summary & conclusion

To summarize, the phase behavior of mixtures of polyoxacyclobutane $-[CH_2CH_2CH_2O-]_n$ and water combines two features. First, POCB and water cocrystallize in a 1:1 ratio of monomer to water to form a hydrate; this appears to be one of only two polymers that form a crystalline hydrate. Second, upon melting the hydrate, the mixtures phase-separate into a POCB-rich and water-rich phase in LLE. To our knowledge, no other polymer-small molecule pair shows such phase behavior combining cocrystallization and LLE.

Due to the nature of this phase diagram, POCB hydrate crystallization can initiate either from a homogenous liquid state, or from a LLE state. Previously we examined the kinetics of hydrate crystallization from a homogeneous liquid state. Here we continue with kinetic studies of hydrate crystallization from the LLE state.

We developed a novel method to measure the speed of hydrate spherulite growth in mixtures under isothermal LLE conditions. Mixtures in LLE were placed in a petridish so that the POCB-rich droplets deposited onto the bottom of the dish to form puddles submerged under the water-rich phase. Spherulites grew within these puddles and were imaged by optical microscopy. The resulting growth speed was found to be invariant with time as the growth front propagated across the puddles. We believe that this is because such puddles have access to a large excess of water in the surrounding water-rich phase. In contrast, in our previous studies of hydrate crystallization from a homogeneous liquid state, depletion of the POCB near the interface reduced the speed of spherulite growth as spherulites grew. The spherulite growth speed in the puddles increased with increasing undercooling in a manner consistent with the Hoffman Lauritzen model. The temperature-dependence of the speed measured for crystallization from LLE was very similar to that measured here and previously [4] for crystallization from the homogenous state.

Isothermal bulk crystallization kinetics were measured by dilatometry with continuous stirring. Since water and POCB are both necessary for hydrate crystallization, good mixing is essential; without stirring, crystallization proceeded very slowly due to gravitationally induced layering of the two liquids due to their density difference. Continuous stirring also ensures that there are no composition gradients in the bulk liquids as crystallization proceeds. Similar to spherulite growth speed, the bulk crystallization of stirred samples were also found to accelerate with increased undercooling, but with a far weaker temperature

dependence than spherulite growth speed. Finally, we also noted a significant effect of polydispersity: Low molecular weight POCB is fully soluble in water, and our experiments on polydisperse POCB of MW 650 g/mol suggest that this soluble fraction can crystallize as a hydrate from the water-rich phase onto the surface of the POCB-rich hydrate domains. Such crystallization from the water-rich phase is likely responsible for endowing each POCB-rich domain with a corona of crystals.

We close by noting that numerous examples of cocrystallization of polymers with small molecule compounds are known, but there is very little knowledge of cocrystallization kinetics in those systems. For instance, basic questions such as whether cocrystal spherulites grow at constant speed, whether their temperature-dependence resembles homopolymer crystallization, and how molecular weight affects crystallization kinetics have not been examined – even without the complication of LLE. Thus, although this paper and our previous research [4] focuses specifically on cocrystallization mixtures of POCB and water, the results are expected to be broadly applicable to other examples of cocrystallization.

5. Method

5.1. Materials

POCB650 was provided by Dupont under the trade name of Cerenol [5]. POCB was mixed with deionized water from a Millipore filter for the bulk crystallization and microscopic experiment.

5.2. Dilatometry

As reported in the previous study [4], bulk crystallization kinetics was measured in dilatometers custom-made by the glass shop of the University of Pittsburgh. All experimental procedures and equipment were identical (ESI Figure S1) to our previous study [4] except that the samples must be stirred during the experiment. Therefore, a magnetic stirrer was added inside of each dilatometer flask. A custom-built setup, which can simultaneously stir five dilatometers using five magnets rotating at the same speed, was placed inside the isothermal water bath. The rotational speed was set to 140 rpm for all the bulk crystallization kinetics experiments.

Mixtures of 20 wt% POCB and 80 wt% deionized water were prepared by weighing the two species directly into the dilatometer flask. The approximate sample weight was 1 g. After preparing the sample, the assembled dilatometer flask and glass tube were kept at a cold temperature overnight to complete the crystallization process. Mineral oil was then added into the flask, and the glass stem of the dilatometer assembled. Sufficient oil was added that the oil meniscus was a few centimeters below the top of the glass stem [4]. The experiments were conducted as described in Section 2.1 and data analysis followed previous [4] procedure.

5.3. Microscopy

For the experiments of Figs. 5 and 6 the sample temperature was controlled with a custom-designed microscope stage wherein circulating cold water flows around and underneath the sample container. The circulating water temperature was maintained by an external chiller (Julabo).

The soluble fraction extracted from POCB650 was found to have a solubility of roughly 5 wt% in deionized water at 40 °C, beyond which the mixtures would turn cloudy indicating LLE. Therefore, the composition of 4 wt% was chosen for the experiments of Fig. 5. The sample was poured into a 20 mL glass vial, sealed with parafilm, and held above 37 °C to melt the hydrate. The resulting homogeneous liquid was then quickly transferred to the microscope stage (Olympus, CKX41 inverted microscope). The images were taken at 3.0 s time intervals using PixeLINK Capture OEM software. The growth of multiple spherulite-like objects could be tracked in a single field of view. The growth speed of these spherical objects was calculated following the previous [4] methodology. The growth speed G and equivalent radius R were calculated from the evolution of area A during spherulite growth using Eq (5). The area of the growing spherulite was measured by converting images into binary form using the ImageJ software [38]. The area was fitted to a polynomial function A(t), and R and G were then obtained from the polynomial using Eq (5). A spherulite growth with time can be found in the Supporting Information Fig. S5).

$$R = \sqrt{\frac{A}{\pi}} \quad \text{and} \quad G = \frac{dR}{dt} = \frac{1}{\sqrt{4\pi A}} \frac{dA}{dt} \qquad \text{Eq 5}$$

For the puddle experiment of Fig. 6, the puddle was formed by spreading a dispersion of the insoluble fraction on the bottom surface of the polystyrene Petri dish. Additional deionized water was added, and the dish sealed with a lid. Before each experiment, the dish was held at approximately 48 °C, which is well above the hydrate melting temperature of 41 °C for the insoluble fraction, for 15–20 min to melt the hydrate completely. It was then quickly transferred to the microscope stage and imaged over time. The linear growth length was tracked from the images using ImageJ software [38]. Then the growth length was plotted against time which ultimately gives the crystallization growth speed on the puddle at a specific temperature.

Notes

The authors declare no competing financial interest.

Funding

This research was supported by the National Science Foundation Award (CBET 1933037).

CRediT authorship contribution statement

Sudesna Banerjee: Methodology, Data curation, Writing – original draft, Software, Validation, Formal analysis, Investigation. **Michael Gresh-Sill:** Methodology, Software, Data curation. **Emily F. Barker:** Writing – review & editing, Resources. **Tara Y. Meyer:** Writing – review & editing. **Sachin S. Velankar:** Supervision, Writing – review & editing, Conceptualization.

Declaration of competing interest

The authors declare that they have no known competing financial interests or personal relationships that could have appeared to influence the work reported in this paper.

Data availability

Data will be made available on request.

Acknowledgments

The authors thank Dr. Hari Sunkara from Dupont for making the POCB available, Dylan Butler for assisting with the design of the dilatometer holder, Maya Roman from Mechanical Engineering Department at the University of Pittsburgh for assisting with design and fabrication of the multi-rotor setup and temperature-controlled microscopy stage, and Zachary Kushnir from Mechanical Engineering Department at the University of Pittsburgh for assisting with the Keyence profilometer microscope to quantify puddle thickness.

Appendix A. Supplementary data

Supplementary data to this article can be found online at https://doi.org/10.1016/j.polymer.2023.126087.

References

[1] H. Kakida, D. Makino, Y. Chatani, M. Kobayashi, H. Tadokoro, Strutural studies of polyethers [-(CH2) mO-] n. viii. polyoxacyclobutane hydrate (modification i), Macromolecules 3 (5) (1970) 569–578.
[2] S. Sasaki, Y. Takahashi, H. Tadokoro, Structural studies of polyformals. II. Crystal structure of poly-1,3-dioxolane: modification II1, J. Polym. Sci. Polym. Phys. Ed 10 (12) (1972) 2363–2378.
[3] Y.T. Hiroyuki Tadokoro, Yôzô Chatani, Hideto Kakida, Structural studies of polyethers, [-(CH2)m-O-]n. V, Polyoxacyclobutane 109 (1967) 96–111.
[4] E.F. Barker, S. Banerjee, T.Y. Meyer, S. Velankar, Liquids that freeze when mixed: homogeneous cocrystallization kinetics of polyoxacyclobutane–water hydrate, ACS Applied Polymer Materials 4 (1) (2022) 703–713.
[5] J. Banerjee, P. Koronaios, B. Morganstein, S.J. Geib, R.M. Enick, J.A. Keith, E. J. Beckman, S.S. Velankar, Liquids that freeze when mixed: cocrystallization and liquid–liquid equilibrium in polyoxacyclobutane–water mixtures, Macromolecules 51 (8) (2018) 3176–3183.
[6] O. Tarallo, Encyclopedia of Polymer Science and Technology, 2002.
[7] J.-M. Guenet, Polymer-solvent Molecular Compounds, Elsevier, 2010.
[8] S. Malik, C. Rochas, M. Schmutz, J.M. Guenet, Syndiotactic polystyrene intercalates from naphthalene derivatives, Macromolecules 38 (14) (2005) 6024–6030.
[9] D. Dasgupta, S. Malik, A. Thierry, J.M. Guenet, A.K. Nandi, Thermodynamics, morphology, and structure of the poly(vinylidene fluoride)−Ethyl acetoacetate system, Macromolecules 39 (18) (2006) 6110–6114.
[10] J.J. Point, C. Coutelier, Linear high polymers as host in intercalates. Introduction and example, J. Polym. Sci. Polym. Phys. Ed 23 (1) (1985) 231–239.
[11] O. Tarallo, V. Petraccone, A.R. Albunia, C. Daniel, G. Guerra, Monoclinic and triclinic δ-clathrates of syndiotactic polystyrene, Macromolecules 43 (20) (2010) 8549–8558.
[12] L.A. Belfiore, C.K. Lee, J. Tang, The influence of competitive interactions on multiple eutectic phase behavior in poly (ethylene oxide) molecular complexes, Polymer 44 (11) (2003) 3333–3346.
[13] L. Paternostre, P. Damman, M. Dosière, Metastabilities of lamellar crystals of molecular complexes, Polymer 39 (19) (1998) 4579–4592.
[14] Y. Chatani, T. Kobatake, H. Tadokoro, Structural studies of poly(ethylenimine). 3. Structural characterization of anhydrous and hydrous states and crystal structure of the hemihydrate, Macromolecules 16 (2) (1983) 199–204.
[15] R. Alamo, J.G. Fatou, J. Guzmán, Crystallization of polyformals: 1. Crystallization kinetics of poly(1,3-dioxolane), Polymer 23 (3) (1982) 374–378.
[16] A. Benkhira, E. Franta, J. Francois, Polydioxolane in aqueous solutions. 1. Phase diagram, Macromolecules 25 (21) (1992) 5697–5704.
[17] H.N. Lee, B.M. Rosen, G. Fenyvesi, H.B. Sunkara, UCST and LCST phase behavior of poly (trimethylene ether) glycol in water, J. Polym. Sci. Polym. Chem. 50 (20) (2012) 4311–4315.
[18] B. Crist, J.M. Schultz, Polymer spherulites: a critical review, Prog. Polym. Sci. 56 (2016) 1–63.
[19] J. Zryd, W. Burghardt, Phase separation, crystallization, and structure formation in immiscible polymer solutions, J. Appl. Polym. Sci. 57 (12) (1995) 1525–1537.
[20] P. Schaaf, B. Lotz, J. Wittmann, Liquid-liquid phase separation and crystallization in binary polymer systems, Polymer 28 (2) (1987) 193–200.
[21] W. Burghardt, Phase diagrams for binary polymer systems exhibiting both crystallization and limited liquid-liquid miscibility, Macromolecules 22 (5) (1989) 2482–2486.
[22] R. Cormia, F. Price, D. Turnbull, Kinetics of crystal nucleation in polyethylene, J. Chem. Phys. 37 (6) (1962) 1333–1340.
[23] R. Richards, The phase equilibria between a crystalline polymer and solvents, Trans. Faraday Soc. 42 (1946) 10–28.
[24] V.I. Harismiadis, D.P. Tassios, Solid−Liquid−Liquid equilibria in polymer solutions, Ind. Eng. Chem. Res. 35 (12) (1996) 4667–4681.
[25] L. Mandelkern, Crystallization of Polymers: Volume 2, Kinetics and Mechanisms, Cambridge University Press, 2004 *(Chapter 11)*.
[26] J.M. Schultz, Roles of 'solute' and heat flow in the development of polymer microstructure, Polymer 32 (18) (1991) 3268–3283.
[27] M. Pracella, Crystallization of Polymer Blends, Wiley, New York, 2013.
[28] Y. Li, B.J. Jungnickel, The competition between crystallization and phase separation in polymer blends: 2. Small-angle X-ray scattering studies on the crystalline morphology of poly(ε-caprolactone) in its blends with polystyrene, Polymer 34 (1) (1993) 9–15.
[29] M. Iwamatsu, Direct numerical simulation of homogeneous nucleation and growth in a phase-field model using cell dynamics method, J. Chem. Phys. 128 (8) (2008), 084504.
[30] L. Mandelkern, Crystallization of Polymers-Chapter 9 second ed., 2nd, Cambridge University Press, New York, USA, 2004 (Kinetics & Mechanism).
[31] R.J.MacElroy, S.Banerjee, S.S.Velankar, Unpublished 2023.
[32] L. Mandelkern, Crystallization of Polymers-Chapter 13 second ed., 2nd, Cambridge University Press, New York, USA, 2004 (Kinetics & Mechanism).
[33] L. Mandelkern, The crystallization kinetics of polymer-diluent mixtures: the temperature coefficient of the process, Polymer 5 (1964) 637–648.
[34] T. Sasaki, Y. Yamamoto, T. Takahashi, Primary nucleation rate and radial growth rate of poly (ethylene oxide) spherulite in viscous solutions, Polym. J. 32 (3) (2000) 263–268.
[35] J.W. Cahn, ON morphological stability of growing crystals, J. Phys. Chem. Solid. (1967) 681. PERGAMON-ELSEVIER SCIENCE LTD.
[36] J.M. Watson, M.G. Baron, The behaviour of water in poly(dimethylsiloxane), J. Membr. Sci. 110 (1) (1996) 47–57.
[37] G.C. Randall, P.S. Doyle, Permeation-driven flow in poly(dimethylsiloxane) microfluidic devices, Proc. Natl. Acad. Sci. USA 102 (31) (2005) 10813–10818.
[38] ImageJ Software. https://imagej.nih.gov/ij/.